Sneutrino identification in dilepton events at the LHC

P. Osland,[a,1] A. A. Pankov,[b,2] N. Paver[c,3] and A. V. Tsytrinov[b,4]

[a]Department of Physics and Technology, University of Bergen, Postboks 7803, N-5020 Bergen, Norway

[b]The Abdus Salam ICTP Affiliated Centre, Technical University of Gomel, 246746 Gomel, Belarus

[c]University of Trieste and INFN-Trieste Section, 34100 Trieste, Italy

Abstract

Heavy neutral resonances appearing in the clean Drell-Yan channel may be the first new physics to be observed at the proton-proton CERN LHC. If a new resonance is discovered at the LHC as a (narrow) peak in the dilepton invariant mass distribution, the characterization of its spin and couplings will proceed via the measurement of production rates and angular distributions of the decay products. We discuss the discrimination of a spin-0 resonance (sneutrino) predicted by supersymmetric theories with R-parity breaking against the spin-1 of Z' bosons and the Randall-Sundrum graviton resonance (spin-2) with the same mass and producing the same number of events under the observed peak. To assess the region of sneutrino parameters (couplings and masses) where the spin determination can be performed to a given confidence level, we focus on the event rate and the angular distributions of the Drell–Yan leptons, in particular using the center-edge asymmetry, $A_{\rm CE}$. We find that although the measured event rate permits solving the above problem partially, the center-edge asymmetry, on the contrary allows to differentiate the various spins entirely with a minimal number of events around 200.

[1]E-mail: per.osland@ift.uib.no
[2]E-mail: pankov@ictp.it
[3]E-mail: nello.paver@ts.infn.it
[4]E-mail: tsytrin@rambler.ru

1 Introduction

One of the first aims of the LHC experiments will be to search for new high-mass resonances in the inclusive Drell–Yan production of dilepton pairs

$$p + p \to l^+ l^- + X \qquad (l = e, \mu), \tag{1.1}$$

where the Fermilab experiments have already pushed the mass limit up to ~ 1 TeV [1,2]. If such a resonance should be found, as a peak in the invariant dilepton mass distribution, it will be crucial to determine its spin. The default assumption would be a spin-1 Z', for which many models have been proposed [3], whereas the more exotic options would be the Randall-Sundrum (RS) spin-2 graviton excitation [4] or a spin-0 scalar. For appropriate values of the relevant coupling constants, these models can lead to the same mass and same number of events under the peak, hence could not be distinguishable from one another from statistics alone. The cases of Z' and graviton, and the perspectives for their discovery and identification, have been extensively discussed in the literature [5], and we shall here focus on the third option, namely a scalar.

The three popular classes of scalars, all hypothetical, are: the Higgs scalar(s), the graviscalars or radions (associated with extra dimensions), and those of supersymmetric theories. While the former two would have a very small branching ratio into a lepton pair, the (scalar) sneutrino could in an R-parity-violating theory be singly produced, and have a non-negligible branching ratio into light leptons, e^+e^- and $\mu^+\mu^-$. This is the case we will study, we will establish in what range of masses and coupling strengths one can distinguish it from a Z' and a heavy graviton at the LHC.

Originally, conservation of $R_p = (-1)^{(2S+3B+L)}$, distinguishing ordinary particles from superpartners, was assumed in supersymmetric extensions of the Standard Model (SM) mainly to avoid fast proton decay. However, since such baryon and lepton-number violating processes can in principle be avoided (or suppressed) also by some other additional symmetries, SUSY models where R-parity violation can to some extent occur are viable and the corresponding phenomenological scenarios have gained considerable interest, see, for example, Refs. [6–8].

For a sneutrino in an R-parity-violating theory, we take the basic couplings to be given by

$$\lambda_{ijk} L_i L_j \bar{E}_k + \lambda'_{ijk} L_i Q_j \bar{D}_k, \tag{1.2}$$

with i, j, k generation indices. Furthermore, L (Q) are the left-handed lepton (quark) doublet superfields, and $\bar{E}$ ($\bar{D}$) are the corresponding left-handed singlet fields. Indeed, due to $SU(2)$ invariance, the sneutrino, which is a $T_3 = +\frac{1}{2}$-member of the doublet, can only couple to a *down*-type quark.

The following facts are important:

- In Drell-Yan dilepton pair production at pp and $p\bar{p}$ colliders, the sneutrino can be produced from a $d\bar{d}$ annihilation in a color singlet state, neither from $u\bar{u}$ nor from initial-state gluons. This is different from the case of a graviscalar.

- There is a wide range of non-excluded coupling strengths, both to the initial-state $q\bar{q}$ pair (λ') and to the final-state dilepton pair (λ). Only the product of these will be relevant to process (1.1), together with the sneutrino width. In fact, they enter via the parameter

$$X = (\lambda'_{i11})^2 \mathrm{BR}, \tag{1.3}$$

where BR is the sneutrino leptonic branching ratio and λ'_{i11} the relevant couplings to the $d\bar{d}$ quarks, with i denoting the sneutrino generation. Among these couplings, λ'_{111} is rather constrained (by neutrinoless double beta decay), whereas λ'_{211} and λ'_{311} could be as large as 10^{-2}–10^{-1} for sneutrinos mass scales in the 100 GeV range [7], and perhaps larger for heavier masses. Similar orders of magnitude at the grand-unification scale are obtained from consideration of neutrino masses [9]. Earlier estimates can be found, e.g., in [10].

We discuss in this paper the perspectives to identify the spin-0 sneutrino contribution to process (1.1) at the LHC, against the spin-1 Z' boson and the spin-2 RS graviton hypotheses, also taking into account the current mass limits from the Fermilab Tevatron. It will be demonstrated that these different cases can to a large extent be sorted out, from an analysis of the total cross sections and angular distributions.

Specifically, in Sec. 2 we will for completeness give a minimum of relevant formulae defining the basic observables used in our analysis. To make the arguments underlying our discussion more transparent, a brief account of the angular distributions characterizing the different models under consideration is given in Sec. 3. In Sec. 4 we define the concept of "confusion region" and discuss our method of spin identification. In Sec. 5 we review the prospects for discriminating any sneutrino from a Z' or a graviton candidate, if some signal were to be found in the 14-TeV data, where we assume a generous sample of 100 fb^{-1}. In Sec. 6 we discuss the early 7-TeV data and low luminosity. Sec. 7 is devoted to a brief discussion of the importance of integrated luminosity, as well as the precision that can be obtained on the sneutrino couplings.

2 Cross sections and angular observables

2.1 Event rates and differential cross sections

The basic experimental observables for discovery of a resonance peak in reaction (1.1) and its spin identification are the total production cross section, governing the event rate:

$$\begin{aligned}&\sigma(pp \to R) \cdot \mathrm{BR}(R \to l^+ l^-) \\ &= \int_{-z_{\mathrm{cut}}}^{z_{\mathrm{cut}}} dz \int_{M_R-\Delta M/2}^{M_R+\Delta M/2} dM \int_{-Y}^{Y} dy \frac{d\sigma}{dM\, dy\, dz},\end{aligned} \tag{2.1}$$

and the lepton differential angular distribution, allowing spin discrimination:

$$\frac{d\sigma}{dz} = \int_{M_R-\Delta M/2}^{M_R+\Delta M/2} dM \int_{-Y}^{Y} \frac{d\sigma}{dM\, dy\, dz}\, dy. \tag{2.2}$$

Here, with M the dilepton invariant mass and M_R the position of the peak: R denotes the three hypotheses for the nature of the observed peak, namely, $R = \tilde{\nu}, Z', G$ for sneutrino, Z' and RS graviton "s-channel" exchange, respectively; $z = \cos\theta_{\mathrm{c.m.}}$ with $\theta_{\mathrm{c.m.}}$ the lepton-quark angle in the dilepton center-of-mass frame and y is the dilepton rapidity. For the full final phase space, the integration limits in Eqs. (2.1) and (2.2) would be $Y = \log(\sqrt{s}/M)$, with s the proton-proton center-of-mass energy squared, and $z_{\mathrm{cut}} = 1$. However, to account for finite angular detector acceptance, $z_{\mathrm{cut}} < 1$ and Y must be replaced by a maximum value $y_{\max}(z, M)$. Concerning the size of the dilepton invariant mass bin ΔM,

we adopt the parametrization of ΔM vs. M proposed in Ref. [11]. Of course, on the one hand, larger ΔM could increase the chance of discovery, and, on the other hand, for an expected narrow peak falling within the bin the signal integral over M should be insensitive to the size of ΔM, whereas the background would increase with ΔM.

To evaluate the event rates and the spin-identification reaches, we shall in Eqs. (2.1) and (2.2) use the CTEQ6.5 parton distributions [12], and convolute them with the partonic cross sections relevant to the different subprocesses under consideration. Also, we shall include K-factors to account for next-to-leading-order QCD effects.

Furthermore, we will impose on the final phase space the constraints specific to the LHC detectors, namely: pseudorapidity $|\eta| < 2.5$ for both leptons assumed massless (this leads to a boost-dependent cut on z [13]); lepton transverse momentum $p_\perp > 20\,\mathrm{GeV}$; reconstruction efficiency of 90% for both electrons and muons [14]. Finally, denoting by N_B and N_S the number of "background" and "signal" events in the ΔM bin, the criterion $N_S = 5\sqrt{N_B}$ or 10 events, whichever is larger, will be adopted as the minimum signal for the peak R discovery.

2.2 Center-edge asymmetry for spin identification

As anticipated above, the z-dependence of Eq. (2.2) is different for sneutrino, Z' and RS graviton exchanges, so that in principle they could be discriminated from each other by performing an angular analysis [15–19]. In practice, this initially requires a boost from the laboratory frame to the dilepton center-of-mass frame on an event-by-event basis. In fact, due to the complete symmetry of the pp initial state at the LHC, the sign of the variable z may not be unambiguously determined for all measured events. To perform the angular analysis we use the *evenly* integrated angular center-edge asymmetry, defined as [20–22]:

$$A_{\mathrm{CE}} = \frac{\sigma_{\mathrm{CE}}}{\sigma} \quad \text{with}$$
$$\sigma_{\mathrm{CE}} \equiv \left[\int_{-z^*}^{z^*} - \left(\int_{-z_{\mathrm{cut}}}^{-z^*} + \int_{z^*}^{z_{\mathrm{cut}}}\right)\right] \frac{\mathrm{d}\sigma}{\mathrm{d}z}\,\mathrm{d}z. \tag{2.3}$$

Here, $0 < z^* < z_{\mathrm{cut}}$ is a priori free, and defines the separation between the "center" and the "edge" angular regions. The actual value of z^* will be "optimized" later in the numerical analysis.

The observable A_{CE}, requiring symmetric z-integration, should by definition minimize the "dilution" implicit in the determination of the sign of z mentioned above. Moreover, as shown by the previous applications of Refs. [21] and [22] to the identification of RS graviton and Z' spins respectively, being based on integrated numbers of events a measurement of A_{CE} could apply to spin identification also in the presence of limited statistics. Finally, being defined by ratios of angular-integrated cross sections, this observable promises to be less sensitive to systematic uncertainties. This is particularly so for the numerical uncertainties related to the K-factor values input in Eqs. (2.1) and (2.2). K-factors show some M-dependence, mostly in the case of gluon-initiated processes through the adopted parton distributions and flattening out for increasing dilepton masses. Moreover, they depend on the chosen definition of the factorization scale vs the renormalization one (the most "popular" - but not unique - choice being $\mu_F = \mu_R = M_{\tilde{\nu}}$). These corrections are expected to cancel to a large extent from the ratio (2.3), and this allows a rather stable

assessment of the minimum number of events necessary for spin-identification of the resonance peak by means of $A_{\rm CE}$, which is our main purpose here. Numerical attempts with different sets of parton distributions and K-factors essentially confirm this expectation. Conversely, the mentioned ambiguities on K-factors may directly affect the theoretical predictions for total production rates and discovery reaches, for example needed for the determination of sneutrino couplings from data, and within the partial cancellations found among the different kinds of corrections, can amount cumulatively to a 10% uncertainty.

We mention, in this regard, that spin-diagnostics for s-channel produced resonances in the process (1.1), based on the analogous center-edge asymmetry $\tilde{A}_{\rm CE}$ defined in terms of differences between the lepton and the antilepton pseudorapidities, have recently been successfully applied in Ref. [23]. Also, graviton spin-2 identification from the azimuthal angular dependence of graviton+jet inclusive production followed by graviton decaying into a dilepton pair has been attempted in [24].

3 Model parameters and angular distributions

As anticipated in the Introduction, the detection of a peak at some $M = M_R$ may not be sufficient to identify the non-standard interaction causing it. Indeed, different scenarios can in certain domains of the relevant coupling constants give the same number of events under the peak at M_R, in which case the spin identification is crucial. In this regard, for any model we define as *discovery* reach the upper limit of the resonance mass range M_R for which a signal can be observed (generally, at 5 σ), and as *identification* reach the largest M_R for which the *spin* can be identified at a chosen confidence level. In our case, the spin-0 identification reach on the sneutrino will be determined by the minimal number of signal events allowing to exclude both the spin-1 *and* the spin-2 hypotheses. Of course, both the discovery and the identification reaches depend, among other things, on the energy and luminosity at the LHC. We now briefly expose the main features of the three models, in particular we introduce the notations for the coupling constants relevant to our discussion and their current experimental limits.

3.1 R-parity violating sneutrino and discovery reach

In this case the relevant leading order quark-initiated process is $d\bar{d} \to \tilde{\nu} \to l^+l^-$, and for the explicit leading-order expression of the cross section we refer to [6]. Basically, the cross section depends on the exchanged sneutrino mass $M_{\tilde{\nu}}$ and the R-parity breaking parameter X defined in Eq. (1.3). Present 95% CL lower limits on the sneutrino mass vary from $M_{\tilde{\nu}} > 397\,{\rm GeV}$ for $X = 10^{-4}$ to $M_{\tilde{\nu}} > 866\,{\rm GeV}$ for $X = 10^{-2}$ [1]. The upper value of X, of the 10^{-2} order, reflects the bounds of order 10^{-1} on λ'_{211} and λ'_{311} mentioned in the Introduction, while the lower value, 10^{-4}, is fixed by the experimental sensitivity obtainable at the Tevatron.

Current constraints on X (and λ's) for TeV sneutrino masses are very loose, and we will consider the broad interval $10^{-5} \leq X \leq 10^{-1}$, which would correspond to rather larger values of λ'_{ijk}, as given by Eq. (1.3) and shown in Fig. 1 for the range of branching values $0.01 \leq BR \leq 1$. The trilinear leptonic couplings of the sneutrino, λ_{ijk}, are rather model dependent, and therefore not specified. On the other hand, our main interest here lies in the spin-0 scalar exchange identification vs alternative spin exchanges, rather

than in λ' determinations, and in this regard our analysis should be considered as model-independent.

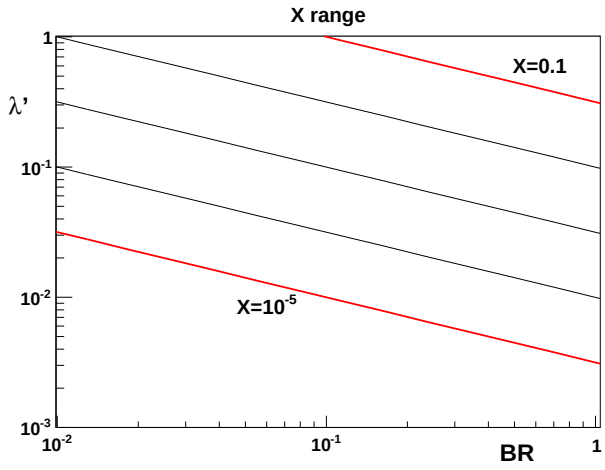

Figure 1: Explored range of X vs branching ratio BR. Contours for $X = 10^{-5}$, 10^{-4}, 10^{-3}, 10^{-2} and 0.1.

The z-even dependence of (2.2) needed in Eq. (2.3) can symbolically be written in self-explanatory notations as:

$$\frac{\mathrm{d}\sigma^{\tilde{\nu}}}{\mathrm{d}z} = \frac{3}{8}(1+z^2)\sigma_q^{\mathrm{SM}} + \frac{1}{2}\sigma_q^{\tilde{\nu}}, \tag{3.1}$$

and at the peak $M = M_{\tilde{\nu}}$ the spin-0 character implies a flat angular distribution. The subscript 'q' here indicates the $q\bar{q}$-initiated parton subprocess. Concerning the center-edge asymmetry:

$$A_{\mathrm{CE}}^{\tilde{\nu}} = \epsilon_q^{\mathrm{SM}}\, A_{\mathrm{CE}}^{\mathrm{SM}} + \epsilon_q^{\tilde{\nu}}(2z^* - 1). \tag{3.2}$$

Here, $\epsilon_q^{\tilde{\nu}}$ is the fraction of $q\bar{q} \to \tilde{\nu} \to l^+l^-$ events, depending on overlaps of partonic distributions, and ϵ_q^{SM} is defined analogously, with $\epsilon_q^{\tilde{\nu}} + \epsilon_q^{\mathrm{SM}} = 1$. Strictly speaking, Eqs. (3.1) and (3.2) and the analogous subsequent expressions for the cross sections for the Z' and graviton cases, hold exactly in the limit $z_{\mathrm{cut}} = 1$, whereas we shall impose $z_{\mathrm{cut}} = 0.98$. It turns out that the difference is numerically unimportant at the values of z^* at which the spin-identification analysis will be performed. The numerical results presented in the sequel are obtained from "full" calculations with all foreseen experimental cuts.

The next-to-leading-order K-factors for sneutrino production have been evaluated in Refs. [25–29] and, with inclusion of supersymmetric QCD corrections, in Ref. [30]. We can assume that a flat value $K = 1.30 \pm 0.10$ can represent the various uncertainties mentioned above, and in Fig. 2 we show for this central number the expected 5-σ sneutrino discovery reaches, for the four cases of LHC center-of-mass energy and integrated luminosity anticipated in the Introduction, vs. the R-parity violating parameter X (the e^+e^- and $\mu^+\mu^-$ channels have been combined). In practice, for each line the theoretical uncertainties should be encompassed by an approximately 10% uncertainty band. In the remaining part of the paper we will not represent those bands in order not to make the plots too busy.

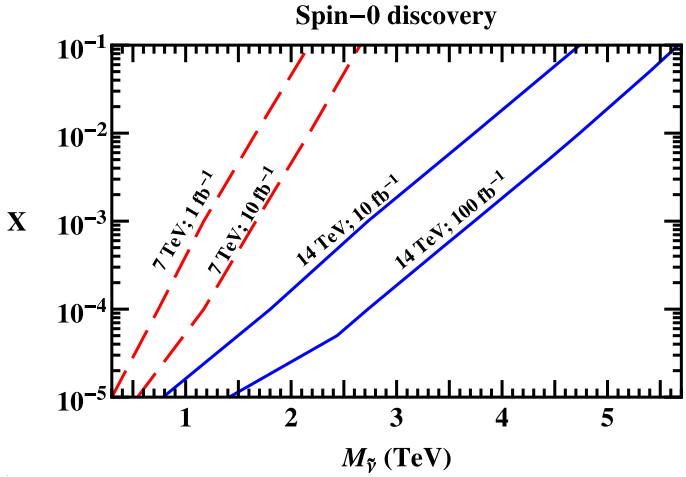

Figure 2: Discovery reach (5-σ level) for sneutrino production at the LHC in process (1.1) at $\sqrt{s}$ =7 TeV, $\mathcal{L}_{\rm int}$ = 1 and 10 fb^{-1} (dashed red lines); $\sqrt{s}$ =14 TeV, $\mathcal{L}_{\rm int}$ = 10 and 100 fb^{-1} (solid blue lines).

3.2 Extra neutral gauge bosons

Extra neutral gauge bosons Z' naturally occur in electroweak models based on extended gauge symmetries, and the leading-order partonic process $q\bar{q} \to Z' \to l^+l^-$ should manifest itself as a narrow peak at $M = M_{Z'}$ with the same form of the z-even differential cross section as for the SM γ and Z exchanges. Thus, the analogues of Eqs. (3.1) and (3.2) read, using the same kind of notations:

$$\frac{{\rm d}\sigma^{Z'}}{{\rm d}z} = \frac{3}{8}(1+z^2)[\sigma_q^{\rm SM} + \sigma_q^{Z'}] \tag{3.3}$$

and

$$A_{\rm CE}^{Z'} \equiv A_{\rm CE}^{\rm SM} = \frac{1}{2}z^*(z^{*2}+3) - 1. \tag{3.4}$$

Note that, contrary to Eq. (3.2), in Eq. (3.4) there is no ϵ characterizing fractions of partonic subprocess events, and, consequently, the value of $A_{\rm CE}$ is for *all* Z' models the same as for the SM. Again, a K-factor value of 1.30 will be assumed for all Z' models [31].

We will here consider the following popular scenarios: Z'_χ, Z'_ψ, Z'_η, $Z'_{\rm LR}$, $Z'_{\rm ALR}$ models, and the "sequential" $Z'_{\rm SSM}$ model with the same couplings as the SM. Although not fully exhaustive of the rather numerous multitude of Z' models, the considered list should nevertheless be sufficiently representative of the different extended gauge electroweak symmetries underlying such scenarios. A common feature of the chosen models is that the Z' couplings to leptons and quarks are there fixed to well-defined numerical values. As will be seen below, in Figs. 4–6, the considered range of couplings is for Z' models much more constrained than for the sneutrino and graviton models. This is caused by assumptions of some kind of unification at high energies. Detailed descriptions and the relevant values of the vector and axial-vector Z' couplings needed for the calculation of the cross sections can be found, e.g., in the reviews [3]. For the chosen Z' models, we list for convenience in Table I the values of the left- and right-handed couplings used in our later plots, and their combinations relevant to the forward-backward-symmetric integration in Eq. (2.3).

Table 1: Left- and right-handed couplings of SM fermions to the Z' gauge bosons [22].

fermion	e			u			d		
	$g_{\rm L}$	$g_{\rm R}$	$g_{\rm L}^2+g_{\rm R}^2$	$g_{\rm L}$	$g_{\rm R}$	$g_{\rm L}^2+g_{\rm R}^2$	$g_{\rm L}$	$g_{\rm R}$	$g_{\rm L}^2+g_{\rm R}^2$
Z'_χ	0.70	0.23	0.54	−0.23	0.23	0.11	−0.23	−0.70	0.54
Z'_ψ	0.30	−0.30	0.18	0.30	−0.30	0.18	0.30	−0.30	0.18
Z'_η	0.19	0.38	0.18	−0.38	0.38	0.29	−0.38	−0.19	0.18
$Z'_{\rm LR}$	0.40	−0.40	0.33	−0.13	0.67	0.47	−0.13	−0.94	0.90
$Z'_{\rm ALR}$	−0.08	−0.05	0.009	−0.01	0.07	0.005	−0.01	−0.02	0.001
$Z'_{\rm SSM}$	−0.64	0.55	0.71	0.82	−0.37	0.81	−1.00	0.18	1.04

Current experimental lower limits on $M_{Z'}$, from the Tevatron collider [1], are model dependent and range from 878 GeV for Z'_ψ to 1.03 TeV for $Z'_{\rm SSM}$ (95% CL). Somewhat higher limits may in principle be obtained in some cases from electroweak precision data, see, e.g., Ref. [32]. Also, attempts to identify Z' couplings, once the spin-1 is established, have been proposed, see for instance Refs. [33–36].

3.3 Graviton excitation from small warped extra dimensions

The simplest version of RS models [4], that addresses the so-called gauge hierarchy problem $M_{\rm Pl} \gg M_{\rm EW}$, consists of one warped extra spatial dimension and two three-dimensional branes at a compactification distance R_c, such that the ordinary SM fields are localized on one brane and gravity originates from the other one and can propagate in the full 5-dimensional space. Due to its peculiar geometry, the model predicts a gravity effective mass scale on the SM brane $\Lambda_\pi = \bar{M}_{\rm Pl} \exp(-k\pi R_c)$, where k is the 5-dimensional curvature and $\bar{M}_{\rm Pl}$ the "reduced" Planck mass $\bar{M}_{\rm Pl} = 1/\sqrt{8\pi G_{\rm N}}$. For $kR_c \simeq 12$, the parameter Λ_π is of the TeV order, hence in the reach of the LHC. The model also predicts a tower of spin-2 graviton excitations, with masses and (universal) coupling constant to SM particles of order Λ_π and $1/\Lambda_\pi$, respectively, that can be exchanged and searched for in the process (1.1) as narrow peaks in M. The phenomenologically most convenient parameterization of the model is in terms of M_G, the mass of the lightest graviton excitation G, and the dimensionless ratio $c = k/\bar{M}_{\rm Pl}$. The theoretically "natural" ranges for the above parameters are $0.01 \leq c \leq 0.1$ and $\Lambda_\pi < 10$ TeV [37].

Recent experimental limits (95% CL) from the Fermilab Tevatron (e^+e^- channel) range from $M_G > 600$ GeV for $c \cong 0.01$ up to $M_G > 1.05$ TeV for $c \cong 0.1$ [2].

The cross sections for the leading-order subprocesses $q\bar{q} \to G \to l^+l^-$ and $gg \to G \to l^+l^-$ read [38,39]:

$$\frac{{\rm d}\sigma^G}{{\rm d}z} = \frac{3}{8}(1+z^2)\sigma_q^{\rm SM} + \frac{5}{8}(1-3z^2+4z^4)\sigma_q^G + \frac{5}{8}(1-z^4)\sigma_g^G, \tag{3.5}$$

and the center-edge asymmetry

$$A_{\rm CE}^{G} = \epsilon_q^{\rm SM}\, A_{\rm CE}^{\rm SM} + \epsilon_q^{G}\left[2\, z^{*5} + \frac{5}{2}\, z^{*}(1 - z^{*2}) - 1\right] + \epsilon_g^{G}\left[\frac{1}{2}\, z^{*}(5 - z^{*4}) - 1\right]. \tag{3.6}$$

Analogous to Eq. (3.2), ϵ_q^G, ϵ_g^G and $\epsilon_q^{\rm SM}$ in Eq. (3.6) are the fractions of resonant G-events for $q\bar{q}, gg \to G \to l^+l^-$ and SM background, respectively, with $\epsilon_q^G + \epsilon_g^G + \epsilon_q^{\rm SM} = 1$. Next-to-leading-order QCD corrections and their uncertainties have been calculated and thoroughly discussed in Ref. [40]. For the subsequent calculations we can take a flat K-factor determination $K = 1.30$, the uncertainty on the total graviton production cross section would be comparable to that for the sneutrino. Once more, the impact of the K-factor on the center-edge asymmetry $A_{\rm CE}$ would be small.

4 Confusion regions and spin identification

As alluded to in the Introduction, the predicted number of events under a peak at $M = M_R$, N_S, can be the same for the different spin hypotheses for values of the respective parameters in specific sets within the domains allowed by current experimental (and/or theoretically natural) limits. For any model, one can define a corresponding *signature space* as the region in the (M_R, N_S) plane that can be "populated" by varying its parameters in the above-mentioned allowed domains. Of course, such domains depend on the LHC energy and integrated luminosity. On the other hand, the *confusion region* for each pair of models is defined as the domain determined by the intersection of the respective signature spaces, where they can give the same number of events and therefore cannot be distinguished from each other by event rates only.

Basically, the procedure we shall use for model identification, specifically the sneutrino identification, goes along the following lines. We assume that a peak is discovered at some value $M = M_R$, and make the further assumption that it is consistent with the spin-0 sneutrino hypothesis, i.e., $R = \tilde{\nu}$. The assessment of the domain in $(M_{\tilde{\nu}}, X)$ where one can exclude the competitor hypotheses, spin-1 and spin-2 with same number of peak events at $M_{\tilde{\nu}}$ and therefore confirm the spin-0 assumption, starts from the deviations

$$\Delta A_{\rm CE}^{G-\tilde{\nu}} = A_{\rm CE}^{G} - A_{\rm CE}^{\tilde{\nu}} \qquad \text{and} \qquad \Delta A_{\rm CE}^{Z'-\tilde{\nu}} = A_{\rm CE}^{Z'} - A_{\rm CE}^{\tilde{\nu}}. \tag{4.1}$$

Figure 3 shows the example of sneutrino exchange with $M_{\tilde{\nu}} = 3$ TeV and $X = 4 \times 10^{-3}$, tested against spin-1 and spin-2 exchanges with the same number of events, at LHC with $\sqrt{s} = 14$ TeV and $\mathcal{L}_{\rm int} = 100$ fb^{-1} [$l = e, \mu$ combined], vertical bars are 1-σ statistical uncertainties. The figure shows that $A_{\rm CE}$ at $z^* \simeq 0.5$ indeed discriminates the three spin hypotheses at the assumed luminosity, and indicates that the maximum sensitivity to sneutrino can be obtained at this particular value of z^*. Actually, this property persists for all cases considered here, therefore in the remaining part of the paper we shall perform our $A_{\rm CE}$ analysis and present the corresponding results at $z^* = 0.5$.

To define an "estimator" for the minimal number of events needed to exclude the spin-1 and spin-2 hypotheses, we compare the deviations (4.1) with the statistical uncertainty

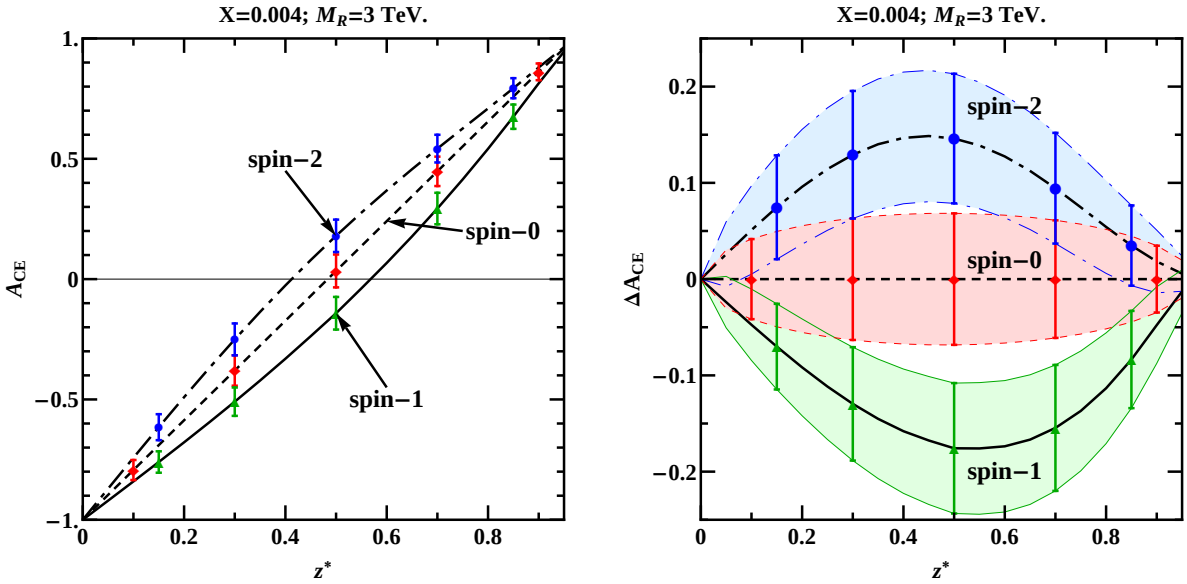

Figure 3: Left panel: $A_{\rm CE}$ vs. z^* for various hypotheses: $\tilde{\nu}$ (spin-0), Z' (spin-1) and G (spin-2) with equal mass of 3 TeV. The error bars attached to the dashed curve are the 1-σ statistical uncertainties on $A^{\tilde{\nu}}_{\rm CE}$ for the sneutrino with $X = 4 \cdot 10^{-3}$ at 100 fb^{-1}. The error bars attached to the solid and dash-dotted curves refer to the spin-1 and spin-2 hypotheses, respectively, assuming the same number of resonance events as for the sneutrino case. Right panel: corresponding $A_{\rm CE}$ deviations of Eq. (4.1).

on $A^{\tilde{\nu}}_{\rm CE}$ (systematic uncertainties can also be accounted for in this analysis):

$$\delta A^{\tilde{\nu}}_{\rm CE} = \sqrt{\frac{1-(A^{\tilde{\nu}}_{\rm CE})^2}{N_S}} \approx \sqrt{\frac{1}{N_S}}. \tag{4.2}$$

(Numerically, $(A^{\tilde{\nu}}_{\rm CE})^2 \ll 1$ at $z^* \simeq 0.5$.) We apply simple-minded χ^2-like conditions to determine $N_{\rm min}$ for exclusion of the two competing hypotheses, respectively:

$$|\Delta A^{G-\tilde{\nu}}_{\rm CE}|^2 = \kappa |\delta A^{\tilde{\nu}}_{\rm CE}|^2; \qquad |\Delta A^{Z'-\tilde{\nu}}_{\rm CE}|^2 = \kappa |\delta A^{\tilde{\nu}}_{\rm CE}|^2. \tag{4.3}$$

Here, κ is a critical value that defines the confidence level, we take $\kappa = 3.84$ for 95% CL. Also, $N_{\rm min}$ can be different in order to exclude the spin-1 or the spin-2 hypothesis from the spin-0 assumption, the larger minimal number of events will be the one needed for the exclusion of *both* competitor scenarios. In Eq. (4.3), $\Delta A^{G-\tilde{\nu}}_{\rm CE}$ and $\Delta A^{Z'-\tilde{\nu}}_{\rm CE}$ of Eq. (4.1) can be expressed in terms of the resonance mass M_R and coupling constants (X, c) with the help of Eqs. (3.2), (3.4) and (3.6). Then, the condition (4.3) will define the domains in the confusion-region planes of model parameters defined above, where the spin-0 hypothesis can be discriminated from the others by using the observable $A_{\rm CE}$. In the next sections we show the signature spaces and confusion regions relevant to the LHC running conditions anticipated in the Introduction, taking into account the current experimental and "theoretical" limits exposed above.

5 LHC nominal energy, high luminosity

Starting from the case $\sqrt{s} = 14$ TeV, and high luminosity $\mathcal{L}_{\rm int} = 100\,{\rm fb}^{-1}$, the sneutrino signature space in (M_R, N_S) is represented by the full area bounded by the solid curves labelled as $X = 10^{-5}$ and $X = 10^{-1}$ in Fig. 4, where the relevant phase space cuts specified above have been applied and the long-dashed line represents the minimum signal for resonance discovery at 5σ above the SM "background".

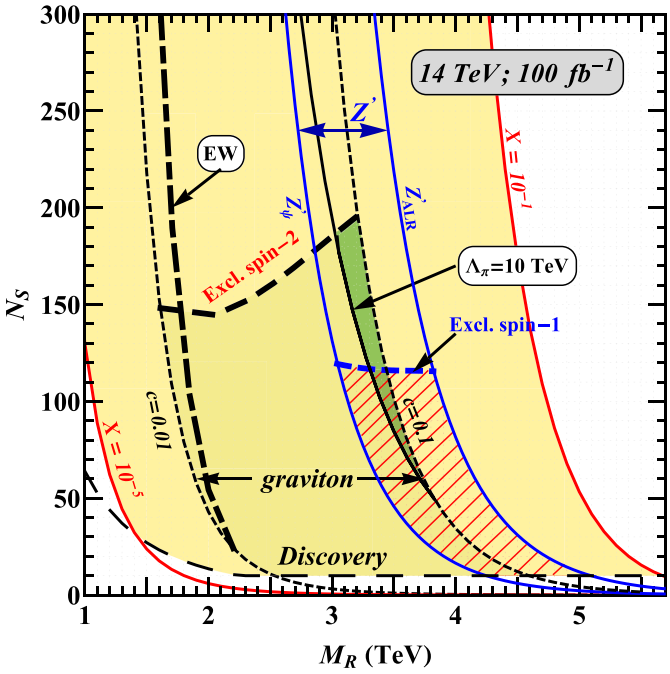

Figure 4: Number of resonance (signal) events N_S vs. M_R ($R = \tilde{\nu}_\tau, Z', G,$) at the LHC with $\mathcal{L}_{\rm int} = 100$ fb^{-1} for the process $pp \to R \to l^+l^- + X$ ($l = e, \mu$). Yellow area corresponds to the sneutrino signature space for $10^{-5} < X < 10^{-1}$. The graviton signature space for $0.01 < c < 0.1$ and event rates for various Z' models are also shown. Minimum number of signal events needed to detect the resonance above the background at the 5-σ level (long-dashed curve) and the minimum number of events to exclude the spin-2 and spin-1 hypotheses in favor of the spin-0 one, assuming spin-0 is true, at 95% C.L., are shown. Regions of confusion are indicated: for sneutrino and graviton (green); for sneutrino and Z' bosons (hatched).

In turn, the signature space for the lightest graviton RS excitation G is represented by the domain constrained by the curves "$c = 0.01$" and "$c = 0.1$". However, the portion lying to the left of the curve labelled as $\Lambda_\pi = 10$ TeV is theoretically disfavored. The curve "EW", also depicted in this figure, represents the constraint on (M_G, c) from EW oblique corrections [37, 41], but is subject to assumptions on the high-energy structure of the theory. The region to the left is "forbidden".

Finally, the signature space of the considered Z' models is the (rather narrow) area delimited by the curves labeled "$Z'_{\rm ALR}$" and "Z'_ψ". Actually, being characterized by coupling constants that are numerically fixed, all of the Z' models considered here are represented simply by curves in the (M_R, N_S) plane. In order not to make the figure too busy, we represent just the leftmost and rightmost Z' lines, the others lie inside that

domain. Tevatron experimental limits on masses lie around (or below) 1 TeV and are not reported in this figure.

In practice, in Fig. 4, the $X = 10^{-5} - 10^{-1}$ sneutrino domain is so wide as to fully include the Z' signature space and, in turn, the latter fully includes the RS resonance signature space if the restriction from the Λ_π line is strictly applied. From Fig. 4 one can easily read off the domain in $(M_{\tilde{\nu}}, X)$ where, for example, the RS graviton exchange within its allowed parameter range can mimic sneutrino exchange by the same number of signal events, as well as the domain where sneutrino exchange can similarly be confused with that of a Z'. The intersection domain of the three signature spaces is the confusion region where the number of events, $N_S(pp \to \tilde{\nu} \to l^+l^-) = N_S(pp \to Z' \to l^+l^-) = N_S(pp \to G \to l^+l^-)$ ($l = e, \mu$ combined), and the three spin hypotheses cannot be distinguished from each other from event rates only. Of course, outside the confusion regions, the various scenarios *may* be mutually distinguished from one another on the basis of the number of signal events N_S, and the corresponding domains can be readily read off from Fig. 4. For example, events falling to the right of the line "$Z'_{\rm ALR}$" can unambiguously be identified as sneutrino exchange, and the same is true for those to the left of the "Z'_ψ" line (where we also rely on the Λ_π constraint); conversely, events between the "$c = 0.1$" and "$Z'_{\rm ALR}$" lines can be confused as either sneutrino or Z' events, those between the "Λ_π" and "$c = 0.1$" curves can be either RS graviton or Z' or sneutrino exchange.

The line labelled "Excl. spin-2" represents the application of angular analysis, specifically the $A_{\rm CE}$ condition (4.3), to the determination of the minimum number of events needed for the 95% CL exclusion of the spin-2 RS graviton hypothesis by the spin-0 sneutrino assumption for the observed peak at $M = M_R$ (here, the condition $\Lambda_\pi < 10$ TeV has been relaxed). A larger (or equal) number of events than represented by that curve is therefore needed to that purpose. Analogously, the curve labelled as "Excl. spin-1" corresponds to the minimal number of events necessary to exclude the spin-1 Z' hypothesis once the sneutrino spin-0 scenario has been assumed as true. For N_S below these curves, confusion regions between the models still remain, which are marked in the figure.

Accordingly, Fig. 4 indicates that the identification of the sneutrino against the RS graviton by angular analysis requires for $M_{\tilde{\nu}}$ in the range from about 1.6 to 3.2 TeV, a minimum of 150-200 events (200 events if one strictly applies the condition $\Lambda_\pi < 10$ TeV). The exclusion of the considered Z' models in the confusion dilepton mass range can be obtained with a minimum of about 120 events. The full identification of a sneutrino can finally be determined by the exclusion of both, namely, by the larger of these numbers. The complete sneutrino identification domain in the $(M_{\tilde{\nu}}, X)$ plane at $\sqrt{s} = 14$ TeV and $\mathcal{L}_{\rm int} = 100\,{\rm fb}^{-1}$ will later be presented, and compared with the case of the same LHC energy, but lower luminosity.

In this analysis, we have adopted a mass-independent K-factor. This is clearly a simplification. In fact, it has been shown that the K-factor is larger than 1.3 at low masses, but then falls with increasing sneutrino mass [25, 28–30]. For the considered asymmetry, $A_{\rm CE}$, this effect cancels out, but it does affect the overall number of events, and hence the discovery limit, as discussed above.

6 Lower luminosity and energy

6.1 LHC nominal energy and lower luminosity

The panels in the left column of Fig. 5 represent the signature spaces for sneutrino, Z' and RS graviton exchanges at the LHC with $\sqrt{s} = 14$ TeV and $\mathcal{L}_{\rm int} = 10\,{\rm fb}^{-1}$. The same experimental cuts as before, and $l = e, \mu$ channel combination, have been applied. The curves enclosing the respective domains are labelled quite similar to Fig. 4, and in particular: the upper panel shows the confusion region between the sneutrino and spin-2 RS hypotheses and the dashed "Excl. spin-2" line gives the minimum number of events required for distinguishing them from each other by the $A_{\rm CE}$ angular analysis; analogously, the middle panel shows the $\tilde{\nu}$–Z's confusion region and the dashed "Excl. spin-1" line is the minimum number of events for a discrimination among them; finally, the lower panel shows the area of total confusion, where all three hypotheses give the same number of events under the peak at M_R. Clearly, compared to the previous case of high luminosity, the sensitivity to sneutrino and its identification via $A_{\rm CE}$ occurs for lower $M_{\tilde{\nu}}$, about 1.9–2.7 TeV, while the minimal number of needed events remains practically the same.

6.2 Lower energy and lower luminosity

In Fig. 5, the panels in the right column represent in complete analogy with those on the left the signature spaces and confusion regions for the initially available LHC energy, $\sqrt{s} = 7$ TeV, and luminosity $\mathcal{L}_{\rm int} = 10\,{\rm fb}^{-1}$. The same phase space cuts (and e, μ channel combination) have been applied as in the preceding sections, and the same notations are used to label the curves delimiting the respective domains. The only difference from the panels on the left discussed above, is that, in the case of the RS graviton, the "EW" constraining curve has considerably approached the "Λ_π" one. We recall that it is the area to the left or below, which is disfavored.

The same kind of conclusions regarding the pairwise confusion regions between the three hypotheses, the overall confusion region and the sensitivity for spin-0 sneutrino identification can be derived. The minimal numbers of events needed for exclusion of the Z' and RS graviton hypotheses by angular analysis are comparable to the previous cases of higher LHC energy, but the relevant values of $M_{\tilde{\nu}}$ are now constrained in the range 1.0–1.7 TeV, approximately, close to (but still above) the current Fermilab Tevatron discovery limits.

It may take some time before the experiments will be able to collect the desirable integrated luminosities of data considered above. In Fig. 6, we plot the signature spaces and confusion regions for $\sqrt{s} = 7$ TeV and the still lower luminosity $\mathcal{L}_{\rm int} = 1\,{\rm fb}^{-1}$, under the same assumptions for the foreseeable experimental cuts on the phase space. The analysis is now complicated by the fact that the relevant masses M_R enter the range of the current Tevatron limits and these, therefore, as shown by the figure, have a significant role in constraining the allowed areas. Basically, one can see that the minimal number of events needed to distinguish the sneutrino from the RS graviton resonance is well above the limit allowed by the Tevatron, see the upper panel. An analogous situation is met for exclusion of some of the Z' models, which are in the middle panel represented in detail by their respective characteristic lines, stopped at the Tevatron lower limits. The application of the angular analysis for spin discrimination in the confusion regions is,

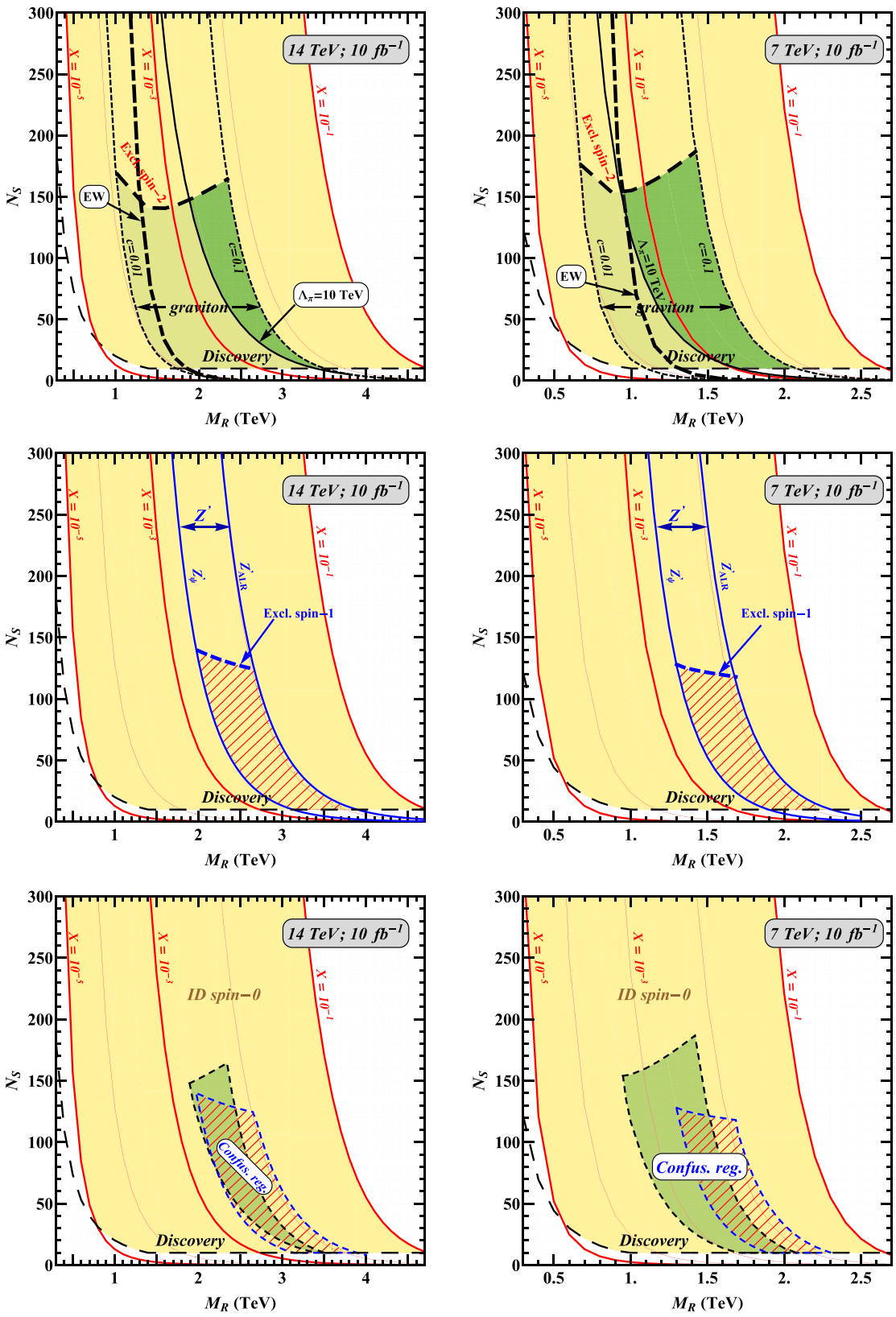

Figure 5: Same as in Fig. 4 but for $\tilde{\nu}_\tau$ vs. G (top panels), $\tilde{\nu}_\tau$ vs. Z' (middle panels) and both combined (bottom panels) at the LHC with $\mathcal{L}_{\rm int} = 10$ fb^{-1}, $\sqrt{s} = 14$ TeV (left column) and $\sqrt{s} = 7$ TeV (right column). Note the different mass scales.

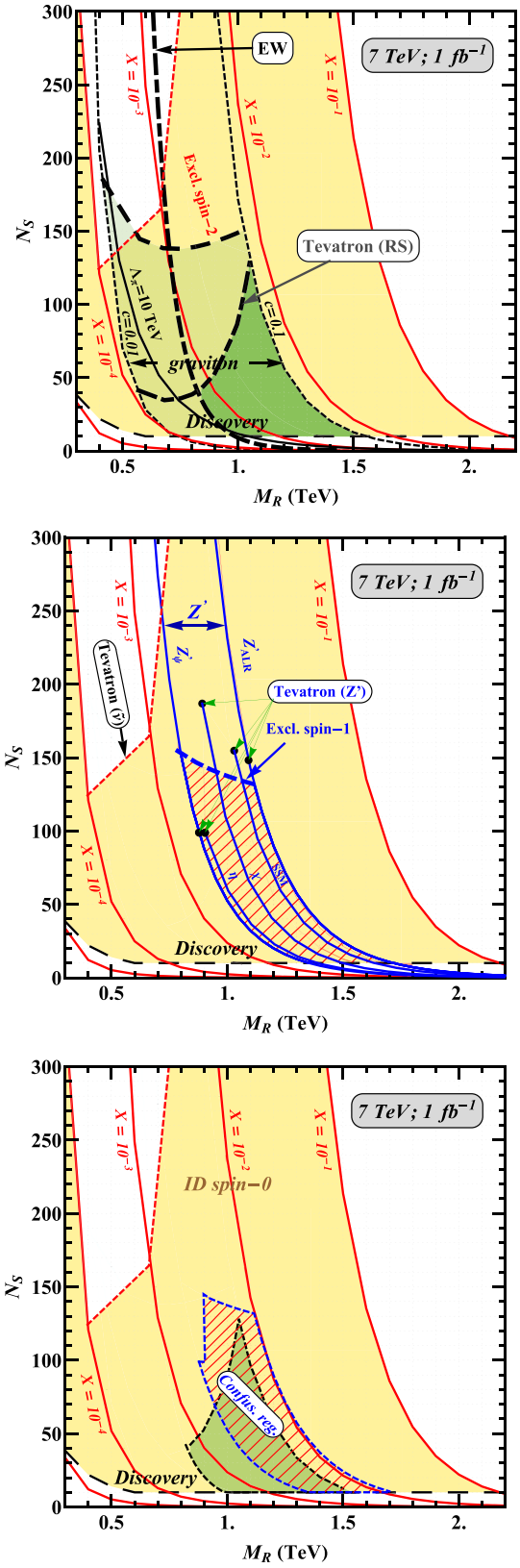

Figure 6: Same as in Fig. 5 but for the LHC with $\sqrt{s} = 7$ TeV and $\mathcal{L}_{\rm int} = 1$ fb^{-1}. Constraints on the signature spaces from the current experimental data are also shown.

accordingly, somewhat problematic in this low-energy and low-luminosity case.

Indeed, the dashed "Excl. spin-2" line in the upper panel in Fig. 6 shows that a minimum of 140 dilepton events should be necessary to discriminate spin-0 from spin-2 by the $A_{\rm CE}$ angular analysis, but this is well above the limits in N_S for the relevant values of $M = M_R$, as set by the curve "Tevatron(RS)". Regarding the discrimination from the Z' hypothesis, the figure in the middle panel, that includes also the current Tevatron limits on the sneutrino mass, shows that for selected values of M_R the spin-0 assumption may indeed be discriminated from some of the Z' models *via* angular analysis, for N_S higher than the "Tevatron(Z')" line. Taking into account the above restrictions from the $A_{\rm CE}$-angular analysis, the sneutrino identification domain in this case is the portion of the sneutrino signature space depicted in yellow in the bottom panel of Fig. 6.

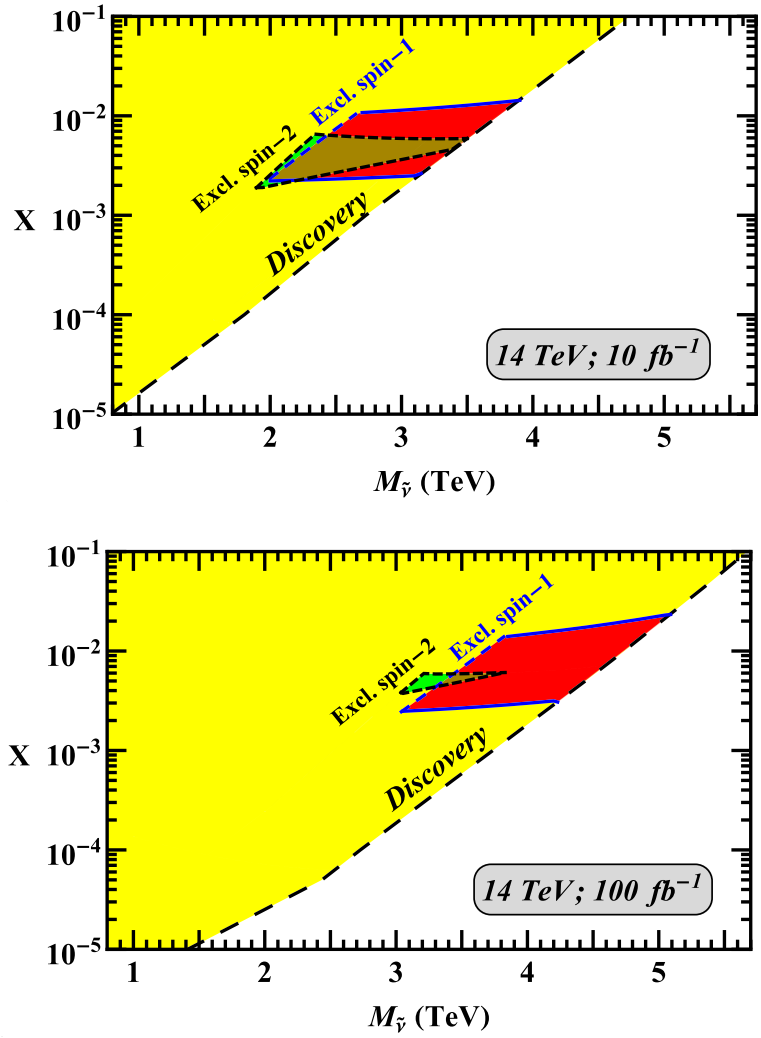

Figure 7: Discovery reach (long-dashed line) and spin-0 sneutrino identification domain (yellow) in the ($M_{\tilde{\nu}}$,X) plane obtained from lepton pair production ($l = e, \mu$) at the LHC with $\sqrt{s} = 14$ TeV, $\mathcal{L}_{\rm int} = 10$ fb^{-1} (top panel) and $\mathcal{L}_{\rm int} = 100$ fb^{-1} (bottom panel), using the production cross section and center–edge asymmetry. The discovery limit is defined by $5\sqrt{N_{SM}}$ or by 10 events, whichever is larger.

7 Luminosity and coupling strength issues

For an assessment of the role of luminosity, we show in the two panels of Fig. 7 the sneutrino discovery and identification reaches in the $(M_{\tilde{\nu}}, X)$ plane for the nominal energy $\sqrt{s} = 14$ TeV and two values of integrated luminosity, $\mathcal{L}_{\rm int} = 10$, and 100 fb^{-1}. The differently colored areas essentially reflect the comments made with regard to Figs. 4 and 5, concerning the confusion and spin-2 and spin-1 exclusion areas determined there.

Specifically, the yellow domain represents the values of $M_{\tilde{\nu}}$ and X for which, if observed as a peak in the process (1.1), the spin-0 sneutrino can unambiguously be identified: referring to the example of Fig. 4, it is composed of the subdomain where identification can be obtained simply from the event rates by themselves, and that where the $A_{\rm CE}$-based angular analysis is needed to perform the discrimination in the confusion regions with the two competitor hypotheses. The trapezoidal and triangular areas (red, brown and green) represent the domains in the sneutrino parameter space where the distinction from both the Z' and the RS graviton hypotheses, cannot be done.

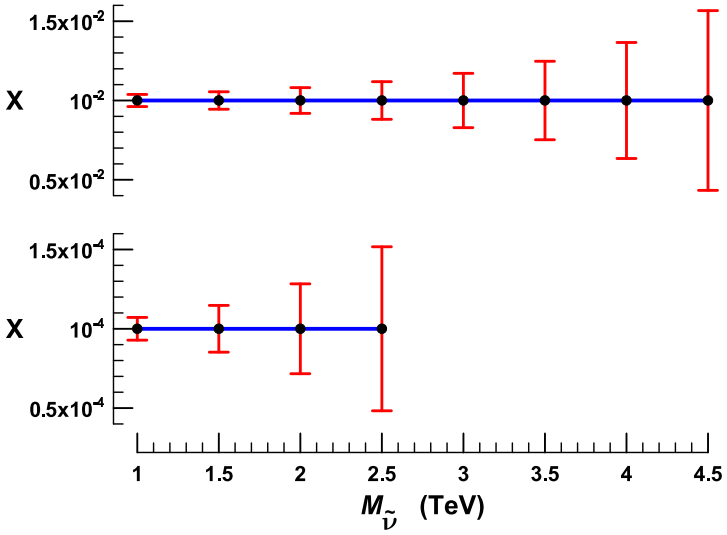

Figure 8: Precision of the spin-0 sneutrino model parameter X for $X = 10^{-2}$ and $X = 10^{-4}$ for increasing $\tilde{\nu}$ mass obtained at the LHC with $\sqrt{s} = 14$ TeV and $\mathcal{L}_{\rm int} = 100$ fb^{-1}.

Assuming that the data is indeed consistent with the spin-0 sneutrino prediction for certain values of $M_{\tilde{\nu}}$ and X, one would also like to know how precisely the parameter X of Eq. (1.3) can be constrained. This question is addressed in Fig. 8, for $\sqrt{s} = 14$ TeV and $\mathcal{L}_{\rm int} = 100$ fb^{-1}, and for two values of X: 10^{-4} and 10^{-2}. The range of sneutrino masses considered, is obviously within the discovery reach, cf. Fig. 2. As the sneutrino mass is increased, the number of events decreases drastically and the statistical fluctuations increase, becoming as large as $|\delta X|/X \approx 0.5$ at the highest masses shown.

In summary, we have determined the regions of mass and coupling strengths for which a sneutrino, if produced resonantly at the LHC, could be distinguished from other candidate resonances such as Z's and Randall–Sundrum excited gravitons. Two energies and three values of the integrated luminosity have been considered. Of the order of 200 events are required for a discrimination against both alternative interpretations in the regions of confusion via the $A_{\rm CE}$-based angular analysis. At the nominal energy of 14 TeV, and

with 100 fb^{-1}, this corresponds to the mass range about 3.0–3.8 TeV, and 1.9–2.6 TeV at 10 fb^{-1}. Outside these mass ranges sneutrino identification can be determined by event rates only.

Acknowledgements
A useful correspondence with Chris Hays is gratefully acknowledged. This research has been partially supported by the Abdus Salam ICTP and the Belarusian Republican Foundation for Fundamental Research. The work of PO has been supported by The Research Council of Norway, and that of NP by funds of MiUR and of University of Trieste.

References

[1] T. Aaltonen *et al.* [CDF Collaboration], Phys. Rev. Lett. **102**, 091805 (2009) [arXiv:0811.0053 [hep-ex]].

[2] V. M. Abazov *et al.* [The D0 Collaboration], Phys. Rev. Lett. **104**, 241802 (2010) [arXiv:1004.1826 [hep-ex]].

[3] J. L. Hewett and T. G. Rizzo, Phys. Rept. **183**, 193 (1989);
A. Leike, Phys. Rept. **317**, 143 (1999) [arXiv:hep-ph/9805494];
T. G. Rizzo, arXiv:hep-ph/0610104;
P. Langacker, Rev. Mod. Phys. **81**, 1199 (2008) [arXiv:0801.1345 [hep-ph]].

[4] L. Randall and R. Sundrum, Phys. Rev. Lett. **83** (1999) 3370 [arXiv:hep-ph/9905221]; **83** (1999) 4690 [arXiv:hep-th/9906064].

[5] For reviews see, *e. g.*, H. Davoudiasl, S. Gopalakrishna, E. Ponton and J. Santiago, arXiv:0908.1968 [hep-ph];
D. E. Morrissey, T. Plehn and T. M. P. Tait, arXiv:0912.3259 [hep-ph];
P. Nath *et al.*, Nucl. Phys. Proc. Suppl. **200-202**, 185 (2010) [arXiv:1001.2693 [hep-ph]].

[6] J. Kalinowski, R. Ruckl, H. Spiesberger and P. M. Zerwas, Phys. Lett. B **406** (1997) 314 [arXiv:hep-ph/9703436]; *ibid.* B **414** (1997) 297 [arXiv:hep-ph/9708272];
T. G. Rizzo, Phys. Rev. D **59** (1999) 113004 [arXiv:hep-ph/9811440].

[7] R. Barbier *et al.*, Phys. Rept. **420**, 1 (2005) [arXiv:hep-ph/0406039].

[8] G. Bhattacharyya and P. B. Pal, Phys. Rev. D **82**, 055013 (2010) [arXiv:1006.0631 [hep-ph]].

[9] H. K. Dreiner, M. Hanussek and S. Grab, Phys. Rev. D **82**, 055027 (2010) [arXiv:1005.3309 [hep-ph]].

[10] See, for example:
G. Bhattacharyya, "A brief review of R-parity-violating couplings," arXiv:hep-ph/9709395; Nucl. Phys. Proc. Suppl. **52A**, 83 (1997) [arXiv:hep-ph/9608415];
H. K. Dreiner, arXiv:hep-ph/9707435, published in *Perspectives on Supersymmetry*,

ed. by G. Kane, World Scientific;
B. C. Allanach, A. Dedes and H. K. Dreiner, Phys. Rev. D **60**, 075014 (1999) [arXiv:hep-ph/9906209];
G. Moreau, M. Chemtob, F. Deliot, C. Royon and E. Perez, Phys. Lett. B **475**, 184 (2000) [arXiv:hep-ph/9910341].

[11] ATLAS Collaboration, Reports No. CERN-LHCC-99-14, CERN-LHCC-99-15.

[12] J. Pumplin, D. R. Stump, J. Huston, H. L. Lai, P. Nadolsky and W. K. Tung, JHEP **0207**, 012 (2002) [arXiv:hep-ph/0201195].

[13] E. W. Dvergsnes, P. Osland, A. A. Pankov and N. Paver, Phys. Rev. D **69**, 115001 (2004) [arXiv:hep-ph/0401199].

[14] R. Cousins, J. Mumford and V. Valuev [CMS Collaboration], Czech. J. Phys. **55**, B651 (2005).

[15] B. C. Allanach, K. Odagiri, M. A. Parker and B. R. Webber, JHEP **0009**, 019 (2000) [arXiv:hep-ph/0006114];
B. C. Allanach, K. Odagiri, M. J. Palmer, M. A. Parker, A. Sabetfakhri and B. R. Webber, JHEP **0212**, 039 (2002) [arXiv:hep-ph/0211205].

[16] R. Cousins, J. Mumford, J. Tucker and V. Valuev, JHEP **0511**, 046 (2005).

[17] O. Antipin and K. Tuominen, Phys. Rev. D **79**, 075011 (2009) [arXiv:0901.4243 [hep-ph]].

[18] F. Boudjema and R. K. Singh, JHEP **0907**, 028 (2009) [arXiv:0903.4705 [hep-ph]].

[19] Y. Gao, A. V. Gritsan, Z. Guo, K. Melnikov, M. Schulze and N. V. Tran, Phys. Rev. D **81**, 075022 (2010) [arXiv:1001.3396 [hep-ph]].

[20] P. Osland, A. A. Pankov and N. Paver, Phys. Rev. D **68**, 015007 (2003) [arXiv:hep-ph/0304123].

[21] P. Osland, A. A. Pankov, N. Paver and A. V. Tsytrinov, Phys. Rev. D **78**, 035008 (2008) [arXiv:hep-ph/0805.2734].

[22] P. Osland, A. A. Pankov, A. V. Tsytrinov and N. Paver, Phys. Rev. D **79**, 115021 (2009) [arXiv:0904.4857 [hep-ph]].

[23] R. Diener, S. Godfrey and T. A. W. Martin, Phys. Rev. D **80**, 075014 (2009) [arXiv:0909.2022 [hep-ph]].

[24] H. Murayama and V. Rentala, arXiv:0904.4561 [hep-ph].

[25] D. Choudhury, S. Majhi and V. Ravindran, Nucl. Phys. B **660**, 343 (2003) [arXiv:hep-ph/0207247].

[26] Y. B. Sun, Y. Jiang, J. R. Huang, L. Han, R. Y. Zhang and W. G. Ma, Commun. Theor. Phys. **44**, 107 (2005) [arXiv:hep-ph/0412205].

[27] L. L. Yang, C. S. Li, J. J. Liu and Q. Li, Phys. Rev. D **72**, 074026 (2005) [arXiv:hep-ph/0507331].

[28] S. M. Wang, L. Han, W. G. Ma, R. Y. Zhang and J. Yi, Phys. Rev. D **74**, 057902 (2006) [arXiv:hep-ph/0609109];
W. Shao-Ming, H. Liang, M. Wen-Gan, Z. Ren-You and J. Yi, Chin. Phys. Lett. **25**, 58 (2008) [arXiv:0706.3079 [hep-ph]].

[29] Y. Q. Chen, T. Han and Z. G. Si, JHEP **0705**, 068 (2007) [arXiv:hep-ph/0612076].

[30] H. K. Dreiner, S. Grab, M. Kramer and M. K. Trenkel, Phys. Rev. D **75**, 035003 (2007) [arXiv:hep-ph/0611195].

[31] M. S. Carena, A. Daleo, B. A. Dobrescu and T. M. P. Tait, Phys. Rev. D **70**, 093009 (2004) [arXiv:hep-ph/0408098].

[32] J. Erler, P. Langacker, S. Munir and E. R. Pena, JHEP **0908**, 017 (2009) [arXiv:0906.2435 [hep-ph]].

[33] M. Dittmar, A. S. Nicollerat and A. Djouadi, Phys. Lett. B **583**, 111 (2004) [arXiv:hep-ph/0307020].

[34] D. Feldman, Z. Liu and P. Nath, JHEP **0611**, 007 (2006) [arXiv:hep-ph/0606294].

[35] F. Petriello and S. Quackenbush, Phys. Rev. D **77**, 115004 (2008) [arXiv:0801.4389 [hep-ph]].

[36] E. Salvioni, G. Villadoro and F. Zwirner, JHEP **0911**, 068 (2009) [arXiv:0909.1320 [hep-ph]].

[37] H. Davoudiasl, J. L. Hewett and T. G. Rizzo, Phys. Rev. Lett. **84** (2000) 2080 [arXiv:hep-ph/9909255];
Phys. Rev. D **63** (2001) 075004 [arXiv:hep-ph/0006041].

[38] T. Han, J. D. Lykken and R. J. Zhang, Phys. Rev. D **59**, 105006 (1999) [arXiv:hep-ph/9811350].

[39] G. F. Giudice, R. Rattazzi and J. D. Wells, Nucl. Phys. B **544**, 3 (1999) [arXiv:hep-ph/9811291].

[40] P. Mathews, V. Ravindran and K. Sridhar, JHEP **0510**, 031 (2005) [arXiv:hep-ph/0506158];
P. Mathews and V. Ravindran, Nucl. Phys. B **753**, 1 (2006) [arXiv:hep-ph/0507250];
M. C. Kumar, P. Mathews and V. Ravindran, Eur. Phys. J. C **49**, 599 (2007) [arXiv:hep-ph/0604135].

[41] T. Han, D. Marfatia and R. J. Zhang, Phys. Rev. D **62**, 125018 (2000) [arXiv:hep-ph/0001320].